Shear-generating motions at various length scales and frequencies in the Baltic Sea – an attempt to narrow down the problem of horizontal dispersion*

OCEANOLOGIA, 46 (4), 2004.
pp. 477–503.

KEYWORDS
Horizontal dispersion
Baltic Proper
Shear-dispersion
Inertial currents

Signild Nerheim

Department of Oceanography,
Gothenburg University,
Box 460, SE–405–30 Göteborg, Sweden;

e-mail: sine@oce.gu.se

Manuscript received 23 July 2004, reviewed 20 August 2004, accepted 4 September 2004.

Abstract

In the Baltic Proper, the mean circulation is too weak to explain the fast southward spreading of the so-called juvenile freshwater trapped by the seasonal thermocline in the summer season. Improved knowledge of the spatial and temporal scales of the velocity field is needed to better model dispersion. Spatial and temporal scales are investigated using some large historic data sets. Inertial oscillations are almost always present in the Baltic Proper, irrespective of wind conditions and mixed layer thicknesses. Analyses of the coherence in one data set reveal that the inertial oscillations have a horizontal coherence scale of 10–20 km under the conditions experienced during those measurements. Transient eddies and basin-scale modes with weaker periodicity are also indicated in our data sets. A tentative wavenumber spectrum is constructed for the Baltic Proper.

1. Introduction

The mechanisms behind the apparently very efficient horizontal large-scale dispersion observed in the surface layers of the sea have eluded disclosure. In the Baltic Proper, for instance, the large volumes of freshwater entering the basin at the coast and from adjacent sub-basins are mixed into the interior continuously. The juvenile freshwater embedded in the

* This work is part of the multidisciplinary project MARE funded by MISTRA.

surface layers is nearly neutrally buoyant, and the observed dispersion is thus comparable to any other dispersion experiment with neutrally buoyant tracers. Theoretical and experimental studies of absolute and relative dispersion have provided knowledge of the statistical properties of dispersion processes, but the coupling between forcing and dispersion is still unclear. In this paper the temporal and spatial scales of motion that may be important for horizontal dispersion are investigated. The investigation is based on various appropriate data sets.

Horizontal dispersion is important for understanding the distributions of pollutants and nutrients and even e.g. plankton, larvae, bacteria and genes. A number of processes contribute to dispersion, which by definition is the spreading of a substance. The only way to durably change the chemical composition of a water parcel is through molecular diffusion. The process is very slow but is enhanced by both turbulent and mean flows, which stretch the material surfaces between water parcels, increasing the surface area over which molecular diffusion can occur. Dispersion occurs through the straining of the surfaces that separate bodies of water with different concentrations of a constituent (e.g. Holt & Proctor 2001).

A number of processes in the sea act to generate the stress and strain fields leading to mixing and dispersion. One of the important processes is turbulence. In fully developed three-dimensional turbulence, the kinetic energy of the turbulent motion in the so-called inertial subrange decays with the wavenumber to the power of 5/3 (Kolmogorov 1941), and the energy is transferred from larger to smaller scales. The inertial subrange ranges from the microscale $\lambda = (\nu^3/\epsilon)^{1/4}$, which depends on viscosity ν and dissipation ϵ, to a length scale L, which describes the scale of the most energetic 3-dimensional motion. Turbulent flows are particularly efficient in creating the stress-strain field necessary for enhanced mixing, given that the strain keeps changing as a result of an ever changing flow field. The length scale L of the largest 3-D motion is limited by either the water depth or the stratification. On scales larger than L, the flow field becomes two-dimensional.

In addition to turbulence, large-scale and tidal currents give rise to current shear which is the important mechanism for dispersion. Sheared currents not only lead to increased turbulence, they also lead to strain at length scales larger than L. This paper is mainly concerned with an exploration of shear-generating motions at various horizontal length scales ($> L$) and frequencies in the Baltic Sea.

Much effort was made on exploration of oceanic dispersion in the 60s and 70s. Joseph & Sendner (1958) performed dye dispersion experiments in the North Sea, postulating a dispersion velocity in a particular version of

the diffusion equation. Experiments demonstrating the shear effect led to simple shear dispersion models. Among these are the model by Bowden (1956), who formulated a model for alternating flow simulating a tidal current and compared it to observations in the Irish Sea, and the simpler one from Okubo & Carter (1966) applicable to similar dispersion problems. Kullenberg (1972) carried out several dye dispersion experiments in coastal and open seas, and proposed that dispersion was caused by vertical current shear together with vertical mixing. Eddy shedding by topography is known to affect dispersion. Increased dispersion caused by island obstacles was observed in a drifter study near Puerto Rico (Sanderson et al. 1995). In a dye experiment in a small lake, dispersion from sources at the coast was found to be slightly faster than dispersion from sources in the central parts of the lake (Lawrence et al. 1995) because of the larger shear in the coastal region. The importance of current shear was further assessed in a laboratory experiment with realistic topography by McClimans & Johannessen (1998), whose findings show that spreading is greatly enhanced by shear dispersion in straits and coastal currents.

On small scales, surface waves have been found to contribute to horizontal dispersion (Schott et al. 1978, Herterich & Hasselmann 1982). Shear flow dispersion mechanisms arising from vertical shear of the internal wave field were modeled by Young et al. (1982). They found that horizontal mesoscale (30 km) stirring takes over from the wave shear mechanism when the length scale of the tracer exceeds 100 m.

Horizontal density gradients can act as barriers to the mixing of objects with buoyancy. Surface drifters were found to converge in a tidal front on Georges Bank, together with seaweed and jetsam (Drinkwater & Loder 2001). Fronts and other structures in the density stratification will affect non-buoyant tracers differently, not necessarily as a barrier, but through the ways in which the density field affects the velocity field, for instance by the formation of baroclinic eddies, or by changing the properties of the surface and internal wave fields.

In principle, it is possible to calculate the dispersion if the velocity field $U(x, y, z, t)$ is known. But, as this never is the case, the common approach is to use dispersion models based on various assumptions regarding dispersion properties, like the eddy diffusion assumption. Attempts at finding a universal dispersion law were made by Okubo (1971), who compiled experimental data from dye and float dispersion experiments. Okubo's empirical laws give relationships between what is called apparent diffusivity and length scale, and between the horizontal variance σ_{rc}^2 of the tracer cloud (treated as symmetric around the mass centre) and time t. The term 'apparent diffusivity' is commonly used for dispersion because

of its analogy to molecular diffusion. The apparent diffusivity can be used in the advection-diffusion equation. Present-day reports on tracer dispersion experiments still make comparison with Okubo's empirical laws (e.g. Lawrence et al. 1995, Peeters et al. 1996, Drinkwater & Loder 2001).

Eilola & Stigebrandt (1998) introduced a new method of observing horizontal dispersion. So-called juvenile freshwater, trapped by the seasonal thermocline in the Baltic Proper, spreads during the summer season with a dispersion rate in accordance with Okubo (1971). This annual experiment is of basin scale dimensions, thus filling the blanks in the larger range of dispersion experiments. The major mechanisms behind the dispersion processes were not found, though spreading by buoyancy driven currents was ruled out. Eilola & Stigebrandt (1998) concluded that the varying wind field is the major agent for horizontal dispersion in the Baltic, as the mean cyclonic circulation is too weak to explain the fast southward transport of juvenile freshwater.

The Baltic (Fig. 1) is a semi-enclosed sea with negligible tides owing to flow restrictions in the Danish straits. The water exchange with the surrounding seas is limited by these relatively shallow and narrow straits. A large volume flow of freshwater enters the Baltic, mainly in the north

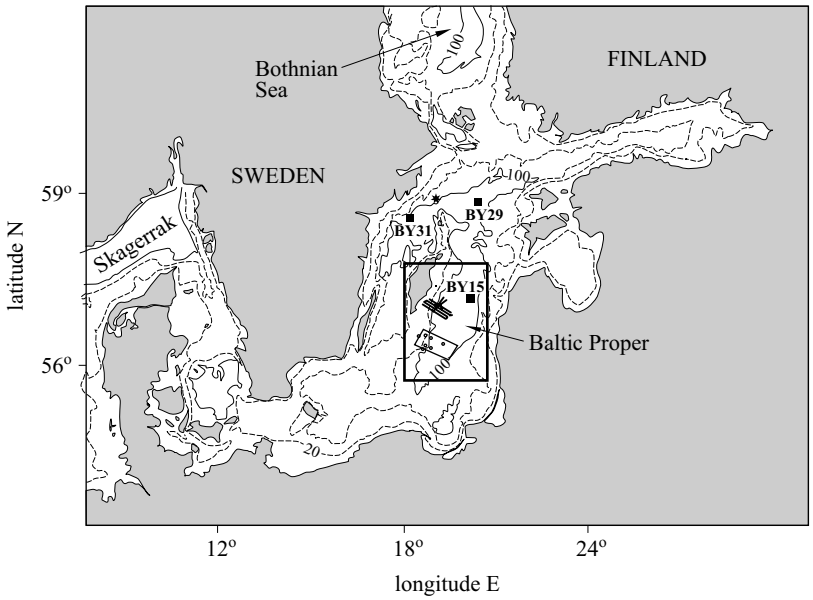

Fig. 1. The Baltic Proper with surrounding seas. The rectangle (Fig. 4) contains the PEX and DIAMIX areas. The star in the north-west is the position of the SMHI buoy. The three main Baltic hydrographic stations, BY15, BY29 and BY31 are indicated as squares

and east from the Bothnian Sea and Gulf of Finland, respectively, while the Polish river Vistula makes the main contribution in the south. All in all, the annual freshwater input ($\sim$15 000 m^3 s^{-1}) is 2% of the volume of the Baltic, and together with the input of salt from the south, the result is a large-scale north-south salinity gradient. Fig. 2 shows the longitudinal section of the Baltic Sea with bottom relief and salinity. A permanent halocline resides at about 60 m depth in the Baltic Proper, and during summer a seasonal thermocline builds up at 15–20 m depth. In the autumn, winds erode the thermocline, and this erosion together with cooling eventually lead to a breakdown, so that a mixed-layer reaching all the way down to the perennial halocline is formed.

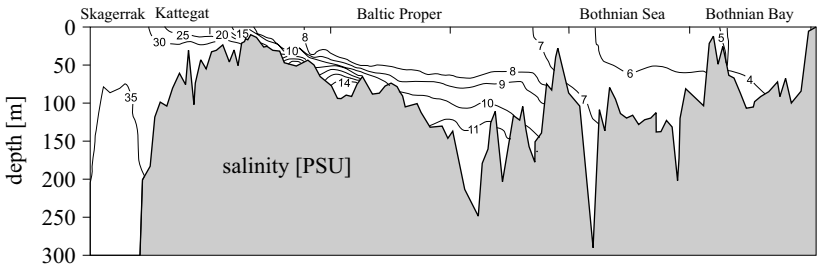

Fig. 2. Transect of the Baltic Proper showing the salinity distribution from the Bothnian Bay to the Kattegat. From Stigebrandt (2001)

The three main Baltic Proper hydrographic stations are BY31 (Landsort), BY15 (Gotland Basin) and BY29 (northern central Baltic Proper). Fig. 3 shows the salinity (upper panel) and temperature (lower panel) measured at 10 m during the ten-year period 1991–2000. The seasonal cycle in temperature is pronounced, and the three stations show a very uniform behaviour. The annual salinity variations are less pronounced, but larger at the northern BY31 and BY29 than at BY15. The instantaneous north-south salinity difference between BY29 and BY15 varies between 0–0.5.

The mean circulation in the upper layer of the Baltic Proper is weak and cyclonic (e.g. Fonselius 1996). Because of the low salinity, buoyancy effects of freshwater in coastal currents are not as important as in other shelf seas. Weak horizontal mean currents, uppwelling and downwelling events, Kelvin waves and mesoscale eddies and topographic waves have all been reported in the Baltic Sea (Fennel et al. 1991, Fennel & Seifert 1995, Lehmann et al. 2002). Stigebrandt et al. (2002) observed inertial currents, near-inertial waves, mesoscale eddies, up-welling and internal seiches at CT and ADCP moorings and vertical CT sections east of Gotland. Raudsepp et al. (2003) looked at low-frequency current variation in the central Gulf of Riga and its dependence on basin-scale topographic wave response. All of the above

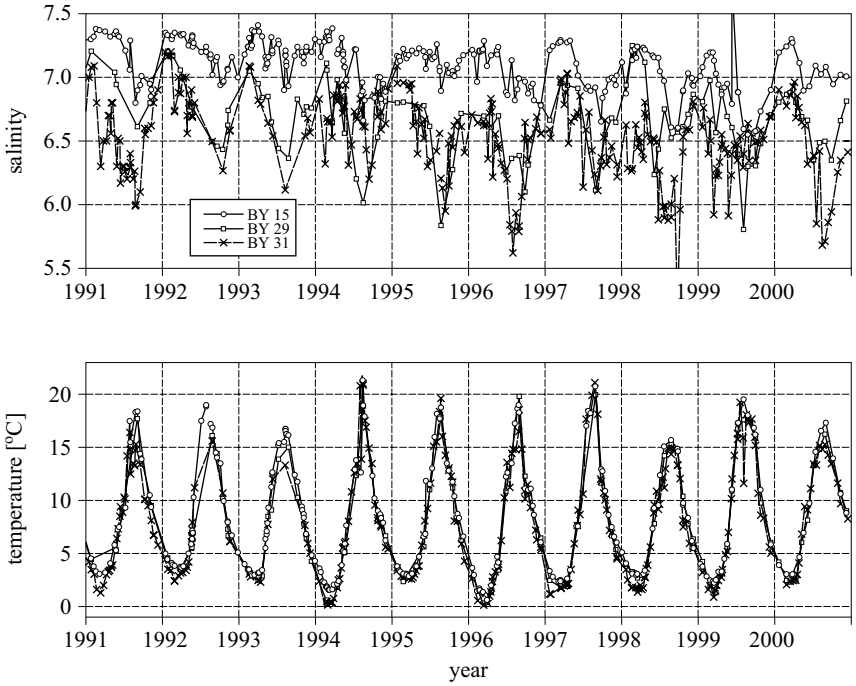

Fig. 3. Salinity and temperature at BY15 (Gotland basin), BY31 (Landsort) and BY29 (northern central Baltic Proper) between 1991–2000. The samples are taken from the mixed-layer, at 10 m depth

mentioned types of motion can be found in most ocean regions and will have different and largely unknown effects on horizontal dispersion.

Although inertial and near-inertial oscillations are common in the Baltic, no comprehensive study has been published. Gustafson & Kullenberg (1933) proposed an e-folding time of a couple of days, while observations from other ocean areas indicate that mixed layer inertial oscillations last for a week or so (e.g. D'Asaro 1989). Liljebladh & Stigebrandt (2000) modeled the inertial currents in the Baltic Proper with a slab model with a damping time scale of 32 hours. The relatively quick damping of wind-driven surface oscillations may be explained by the large frequency-spread of the near-inertial oscillations (Kundu 1976), transport of energy to internal waves in the deeper layers (e.g. Pollard 1970, D'Asaro et al. 1995, Levine & Zervakis 1995), or breakdown caused by a change in wind conditions (e.g. Gustafson & Kullenberg 1933, Pollard 1970).

The non-coherence of the inertial oscillations is a possible source of current shear. Coherence length scales of inertial oscillations are reported to be in the range of tens of kilometers (Kundu 1976). Inertial oscillations in a front (Kunze & Sanford 1984) had a horizontal scale of the order of

10 km. In the Ocean Storms Experiment, two moorings 18.5 km apart were found to have small phase differences (Qi et al. 1995), which means that the inertial oscillations were coherent. In order to obtain correct damping times in a model for the decay of near-inertial waves, the horizontal scale needs to be of the order of 100 km, equivalent to a horizontal wavelength of 600 km (D'Asaro 1989). The scale may be set by wind, horizontal density gradients (Liljebladh & Stigebrandt 2000), oceanic current variability or the β effect.

The aim of this paper is to describe the properties of the velocity field in the Baltic Proper, and discuss them in terms of how they can lead to horizontal dispersion. The dominant frequencies of motion and the length scales connected to them are described. Horizontal gradients in hydrography on large and small lateral scales are presented. Observations are also compared with the analyzed model output from a 3-D eddy-resolving model.

Section two gives a description of the data sets analyzed and the methods involved. The results from velocity measurements are presented in the third section, while those concerning the output from the 3-D model are presented in section four. Section five is a summary and discussion, and this is followed by a short conclusion in section six.

2. Data and methods

2.1. Data

Three datasets of velocity measurements are used in this study, and the places of origin are indicated in Fig. 1. The SMHI buoy in the north-western Baltic Proper provides the three longest time series, which are also the records with the highest resolution in the vertical. ADCP data from the DIAMIX project in the Gotland basin give high-resolution measurements from four different times of the year. Data from PEX, also in the Gotland basin, give information on the current field and its horizontal variations during a period with low winds. The data sets are described in detail below.

SMHI, the Swedish Institute of Meteorology and Hydrology, deploys one buoy at 58°55′N, 19°09′E (star in Fig. 1) in the Baltic Proper on a regular basis. Data from the buoy are current speed and direction, temperature, salinity, wind speed and direction, air pressure and temperature, wave speed and direction and some other parameters. At 2 and 4 m depth, two current meters from Falmouth Scientific Inc. monitors the current, between 12 to 90 m the velocity is measured with an ADP (Nortek, 500 kHz) placed at the bottom. The water depth is 95 m, the sampling rate is hourly. The data has been through a quality control at SMHI. Three periods are analyzed; August–October 2002, June–August 2003 and October–November

2003. The 2002 current data is complete, but the ADCP data from 2003 consists of noise only.

The DIAMIX (DIApycnal MIXing) project aims at investigating wind driven vertical mixing below the pycnocline (Stigebrandt et al. 2002). Two pilot surveys and two main experiments were conducted between June 1997 and September 2000. Inertial currents, near-inertial waves, internal seiches, mesoscale eddies and upwelling were observed in the area during the surveys. The ADCP mooring was placed at 57°08′N, 19°03′E, marked with a circle in Fig. 4. ADCP data from the surface mixed layer from each of the surveys are analyzed. The length of the records vary from 8 to 14 days.

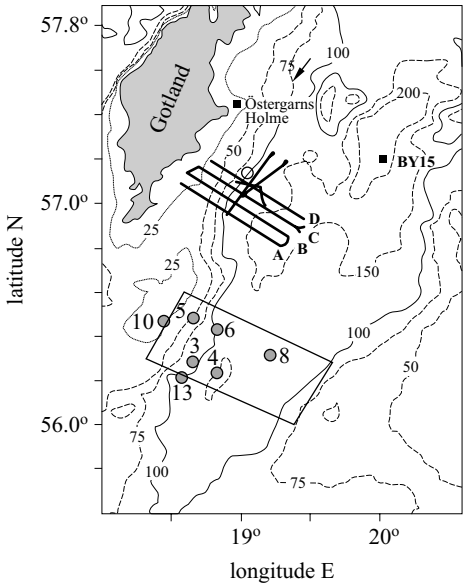

Fig. 4. Map of the PEX (rectangle) and DIAMIX areas. The ADCP mooring from DIAMIX (1997–2000) is the open circle, and the lines show the hydrographic sections measured with an undulating CTD. The seven PEX stations of current measurements analyzed are marked with gray circles

Continuous measurements of hydrographic data were made along 30 nautical-mile-long transects perpendicular to the coast and shorter transects parallel to the coast with vertically undulating vehicles carrying CTDs. Hydrographical data from 1999 measured along tracks crossing the slope (Fig. 4) have been used in the present study, with emphasis on transects labeled A–D.

PEX (The Patchiness EXperiment) was an extensive measurement effort designed to assess the dynamics of patchiness in chemical and biological parameters (ICES 1989). The experiment took place from April 25 to May 8, 1986 in the open parts of the Baltic Proper in the southern part of the eastern Gotland Basin (Figs 1 and 4). 14 ships from seven nations took part (ICES 1989). The current measurements from stations 3–6, 8, 10 and 13 (Fig. 4) were of good quality and are presented below. The current meters at

station 4 were Polish LSK instruments, the remaining stations had current meters from Aanderaa Instruments.

The horizontal gradients in the large-scale density field are mostly due to the north-south salinity gradients. Data from the main Baltic Sea stations BY15, BY29 and BY31 (Fig. 3) are used to assess these gradients.

Wind forcing is important for the motion in the upper mixed layer. At the SMHI buoy, a weather station measured the local wind speed and direction, together with temperature, and a number of other parameters. DIAMIX took place near Gotland, where synoptic wind data from Östergarns holme (Fig. 4) every 3 hours give the wind conditions during the surveys. The PEX report (ICES 1989) describes the atmospheric conditions (including the wind) during PEX in detail.

Model data. Numerical models have long since become much-used tools, where state-of-the-art 3-D models are used both for process studies, hindcast experiments and climate forecasts. Since 3-D models generate data on spatial scales that observations generally cannot confirm, the question is whether the horizontal velocity field computed by a 3-D model mimics the real horizontal velocity field in such a way that one actually knows the velocity field well enough to model dispersion.

Output from the baroclinic, eddy-resolving, coupled sea-ice-ocean model of the Baltic Sea developed by Lehmann (1995) is compared to the measurements at the SMHI buoy. The model has been successful in simulating most of the major Baltic Sea inflows, and has been used e.g. for determining the general circulation of the Baltic Sea, in response to the atmospheric forcing (Lehmann et al. 2002). Current and hydrography data from five adjacent grid cells near the SMHI buoy, the central grid cell being at 58.916°N, 19.15°E, have been analyzed for May–October 2002.

2.2. Methods

Data and filtering. The quality of the data analyzed is generally good. Spikes due to unknown causes have been removed from the SMHI buoy data. Shorter gaps in current and wind data were filled using the simple linear interpolation routine in Matlab. Sections of ambiguous hydrography data have been left out of the analysis.

In order to study directly the measured near-inertial oscillations in the time-series, data were filtered with a bandpass filter to remove the low and high frequencies. A 3rd order Butterworth filter was chosen (e.g. Emery & Thompson 1997), with cut-off frequencies corresponding to 24 and 3 hour periods. Figures of filtered time-series are not shown below, but knowledge gained from filtering is referred to in the text.

Spectral analysis. Since inertial oscillations are an important component in the data, rotary spectral analysis (Gonella 1972, Mooers 1973) was chosen to study the current characteristics in the frequency domain. The velocity vector is decomposed into a positively and a negatively rotating vector, and the energy is found for each rotating vector instead of for the Cartesian components.

Further, following Mooers (1973), the coherence and phase difference between two time series with a horizontal or vertical resolution can be found. This is relevant for the horizontal variations in the PEX data, but can also be used to investigate the vertical phase propagation and coherence.

In spectral analysis, windowing is common. Smoothing spectral estimates increases the degrees of freedom, and narrows the confidence limits. The trade-off is a loss of spectral resolution, and a loss of information on low frequencies. The spectra shown in the paper have all been filtered with a Hanning window with a window length of four days, and an overlap of two. The reason for the short window is that inertial oscillations occur in packages with a duration of 3–4 days, and with a longer window, packages with a random phase lag between them would lead to diminished energy in the spectra. Longer windows have been used to resolve low-frequency motion, and will be referred to in the text.

3. Results

3.1. Buoy data

The SMHI buoy data represent different seasons, with different stratification. The hydrography follow the normal seasonal variations, and none of the periods saw very high winds.

In the first period, August–October 2002, there was a pronounced thermocline at 15–20 m depth in the beginning of the record. It started deepening in early September, and at the beginning of October the thermocline depth was around 32 m, deepening to 40 m. There was a permanent halocline near 60 m, and a seasonal halocline higher up which coincided with the thermocline.

In the second period, June–August 2003, the thermocline was established from the beginning of June. While the temperature increased, the thermocline deepened during June–July, but changed character (a shallower mixed layer and a less sharply demarcated thermocline), and as in the 2002 data, the vertical temperature profile in the upper mixed layer had its mirror image in the salinity. The salinity decreased slowly in this period. The permanent halocline was at 50–60 m.

The third period, October–November 2003, had a well-mixed upper layer, 40 m thick initially. During the last part of October, it deepened to the depth of the permanent halocline in the second half of the month. The temperature decreased during the measurement period.

The buoy measured the local windspeed and direction 3.6 m above the sea surface. The mean wind speed and standard deviation during August–October 2002 were 9 m s^{-1} and 4.6 m s^{-1}. The wind direction was variable, with an emphasis on winds from the north and from west-southwest. In the second period, June–August 2003, winds were markedly lower. The mean wind speed was 5 m s^{-1}, standard deviation 2.6 m s^{-1}. In August, when the wind speeds picked up, northerly and westerly winds were most frequent. In October–November 2003 the mean wind speed was 7 m s^{-1}, and the standard deviation 2.7 m s^{-1}. South-westerly winds were prevalent, but the highest windspeeds (10–15 m s^{-1}) were recorded in October during periods of northerly winds.

Fig. 5 shows the u-component (east-west) of the velocity (cm s^{-1}) from the current meter at 4 m depth from the three records. The 2 and 4 m

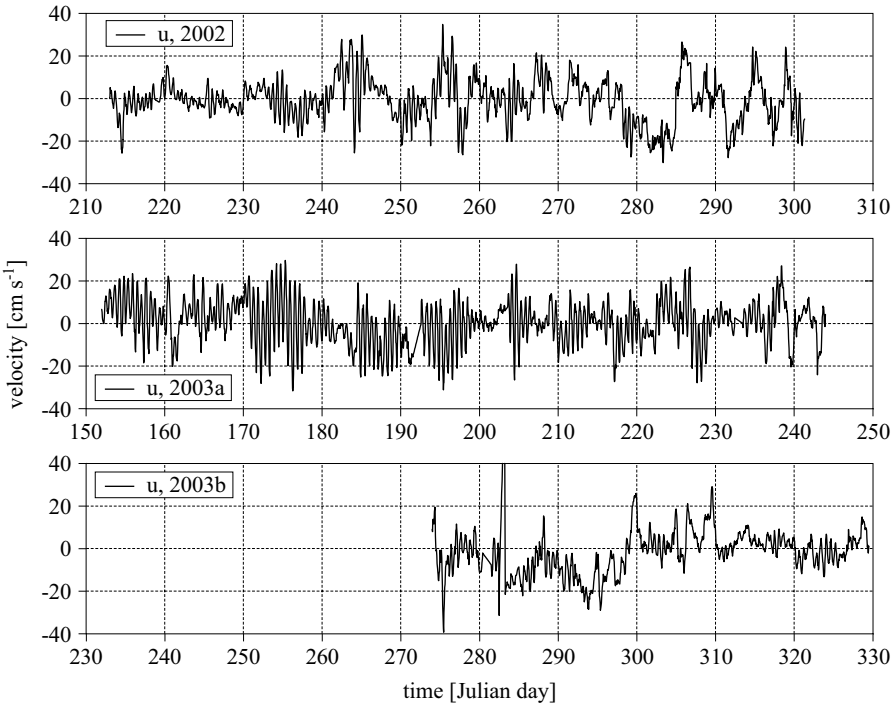

Fig. 5. SMHI buoy current meter measurement at 4 m depth for August–October 2002 (upper panel), June–August 2003 (middle panel) and October–November 2003 (lower panel). The east-west (u-component) is shown

measurements are nearly identical. The v-component from each year is qualitatively similar to the u-component, and is omitted for the sake of clarity. The first period (upper panel) is characterized by inertial oscillations and a slowly varying mean current from around day 240. In this context, the mean current is the velocity on timescales of a day or more. During the second period (middle panel), the mean current is close to zero, and the oscillations are more energetic. The third period (lower panel) is characterized by a much lower energy in the oscillatory motion, and a slowly varying mean current.

Filtered velocities (not shown here) show that the observed oscillatory motion occurs in packages of 5–6 oscillations. Some of the packages merge – a new group of oscillations is sometimes formed before the first group has died out.

Fig. 6 shows the energy spectral density of the positively (cyclonic, solid line) and negatively (anticyclonic, bold line) rotating velocity vector from

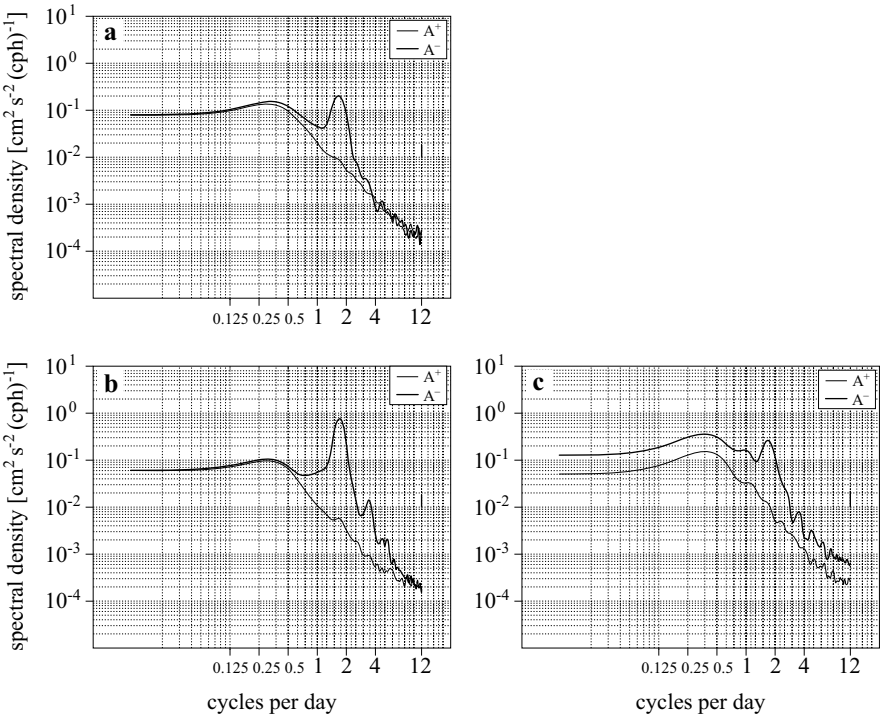

Fig. 6. Rotary spectra from the 4 m depth velocity data from the SMHI buoy, filtered with a 4-day Hanning window. Figure a shows spectra from the 2002 data, b shows the spectra from summer 2003 and c shows the spectra from fall 2003. Bold lines for anticyclonic spectra, solid lines for cyclonic spectra. Vertical bars show the 95% confidence interval for each spectrum

the SMHI buoy data. All three records show a peak in the near-inertial band, near 1.7 cycles per day, for the anticyclonic component. As the amplitude of the oscillations in the filtered time series suggests, the inertial oscillations are more energetic in the summer period (Fig. 6b), and least energetic in the late fall period (Fig. 6c).

The rotary spectra show that the observed oscillations are anticyclonic at the near-inertial frequency – 1.7 cycles per day. The mean energy in the near-inertial motion was strongest during summer 2003, even though the wind was weakest in this period. The integrated total energy of inertial oscillations in the mixed layer, measured by $H\ u^2$, where H is the mixed layer thickness, and u the velocity of the inertial oscillations, shows that summer 2003 also had almost double the total integrated energy compared to the two fall periods, which are comparable. The summer period had a shallow thermocline, and an almost vanishing mean current.

3.2. DIAMIX

The DIAMIX data represent four different time periods over four years; May 1997, January 1998, February 1999 and September 2000. In 1997, the halocline was unusually deep (Stigebrandt et al. 2002), in the subsequent experiment it was found at 60 m depth, which is normal. The summer measurements contained one or more strong thermoclines above the perennial halocline, and in winter very weak stratification in the salinity was found above the halocline. The 10 m wind from stergarns holme (Fig. 3) in 1997 had a mean velocity of 4.2 m s^{-1} (standard deviation 1.7 m s^{-1}). The direction was variable, but the higher winds at the end of the period were westerlies. The winds in January 1998 were higher, with a mean of 5.3 m s^{-1} and a standard deviation of 2.8 m s^{-1}. The direction was west-southwest, backing east during one short period. In February 1999, the mean wind was 7.5 m s^{-1} (standard deviation 2.2 m s^{-1}). This relatively high wind was mainly from west-southwest, veering north toward the end of the period. The September 2000 period also saw high winds, with mean and standard deviations of 7.0 and 2.2 m s^{-1}, respectively. The wind was from the south, veering gradually toward west and north toward the end of the measurement period.

The u-component of the velocity from the ADCP measurements from DIAMIX are shown in Fig. 7. The upper layer moves as one water body, so the chosen depth represents the mixed layer well. There are visible oscillations in the velocity measurements, the amplitudes of the oscillations vary between 10 and 20 cm s^{-1}, which is comparable to the buoy measurements shown in Fig. 5. Wave packages similar to the ones

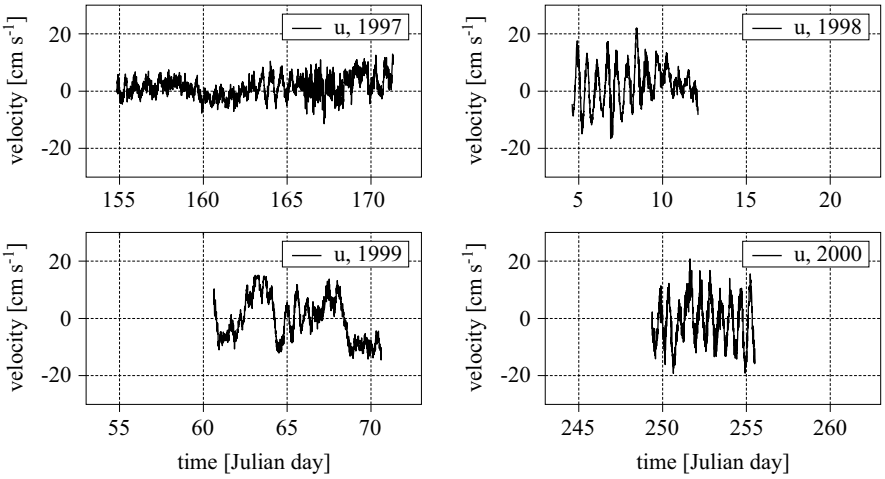

Fig. 7. u-component of the velocity at 10 m depth in the DIAMIX measurements. The measurements are from May 1997, January 1998, March 1999 and September 2000. The time series are plotted with the same scaling on the axes

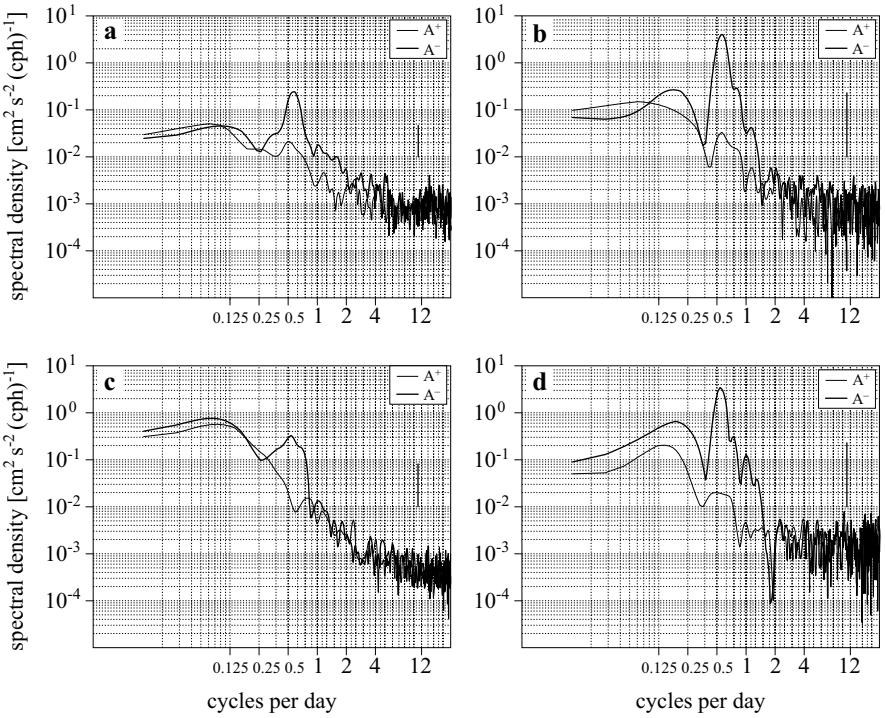

Fig. 8. Rotary spectra from the DIAMIX data, 1997 (a) – 2000 (d). The 95% confidence interval is plotted as a vertical bar

observed at the SMHI buoy are not obvious in the data; however, filtering reveals waves forming and decaying in packages, with the exception of 2000, which is too short for a thorough look at the phenomenon. The 1997 series, which is longest, contains three very clear wave packages.

Fig. 8 shows the rotary spectra from DIAMIX. Inertial oscillations are the dominant feature of the currents, and the energy level is higher than or similar to the energy in the SMHI buoy data. The apparent higher energy at lower frequencies, particularly in the 1999 and 2000 spectra, do not truly represent low-frequency oscillations. Since the window is 4 days long, the lowest possible frequency that can be resolved is 0.5 cycles per day, which means that energy from lower frequencies becomes folded onto that band. Two of the unfiltered spectra (not shown) display a sub-inertial peak, though this is small compared to the confidence interval.

The four transects A–D (Fig. 4) measured with a towed undulating Scanfish-mounted CTD in DIAMIX 1999 provide information on the horizontal salinity field. The measurements in the upper 10 m were binned, and then gridded using the triangular 'griddata'-function in Matlab. The resulting salinity distribution is shown in Fig. 9. The upper left panel shows the salinity on March 2–3, the upper right panel shows the salinity on March 6 (only transects A and B). There is a fresher area in the middle of the transects, and the salinity is higher toward the central Gotland basin in the east. The salinity gradient is approximately 0.05 per km in the area of the highest gradient.

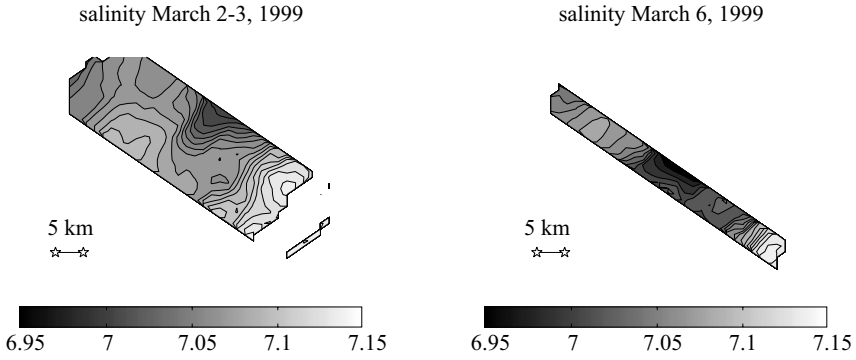

Fig. 9. The salinity at 10 m depth at the DIAMIX sections (north is upwards). The upper left panel is the contour plot from four transects during 18 hours on March 2–3, the upper right panel is the contour plot based on two transects during 8 hours on March 6

The DIAMIX measurements show no tendency toward higher energies in the inertial band in summer than in winter or vice versa. January 1998 was a more energetic year than February 1999, despite the stronger winds

in 1999. The periods differ in that the mean current in January 98 was near zero, whereas the February 99 measurements contained low-frequency motion. September 2000 had more energetic oscillations than May 1997, coinciding with higher wind speeds than in the May record. Perhaps the presence of other components in the May record may have modified the inertial oscillations. The slowly varying mean velocity may have been due to observed mesoscale eddies (Stigebrandt et al. 2002).

3.3. PEX

The hydrograpic conditions during PEX were common for the season, with a weak (1–4°C vertical gradient), 10–15 m thick thermocline in the upper layer (ICES 1989). Hydrography measurements show a persistent front in salinity near the western slope of the PEX area during the whole period. This quasi-permanent front had a maximum gradient of 0.05 per km. The low-salinity waters in the west were separated from the high-salinity water in the east by a body of intermediate salinity. Both the position and gradient of the eastern front were more variable. The two

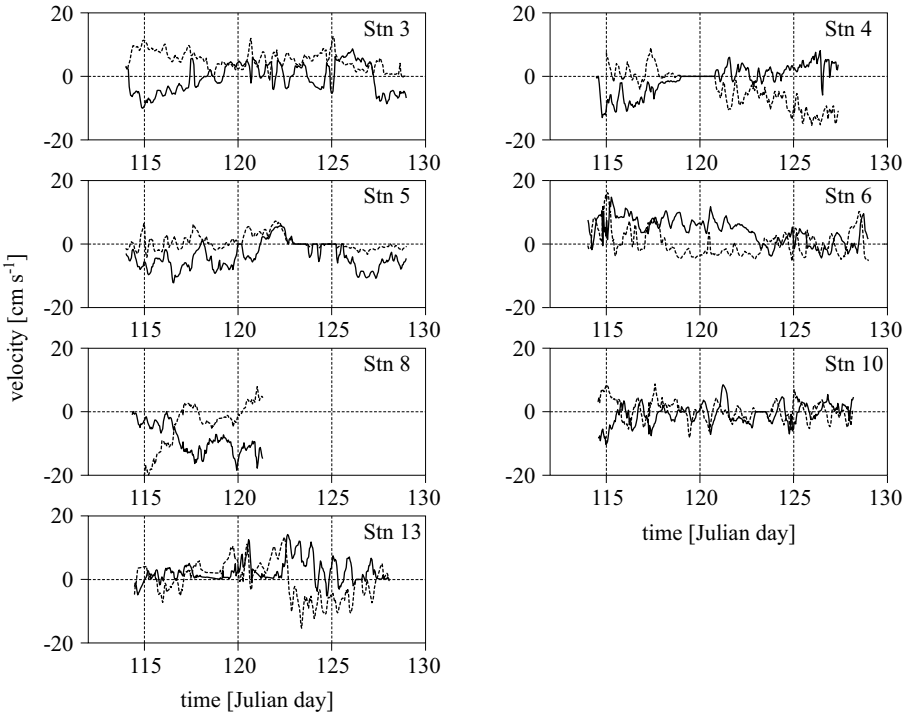

Fig. 10. Velocities, upper layer, from the 7 PEX-stations. u-component, solid line, v-component, dotted line

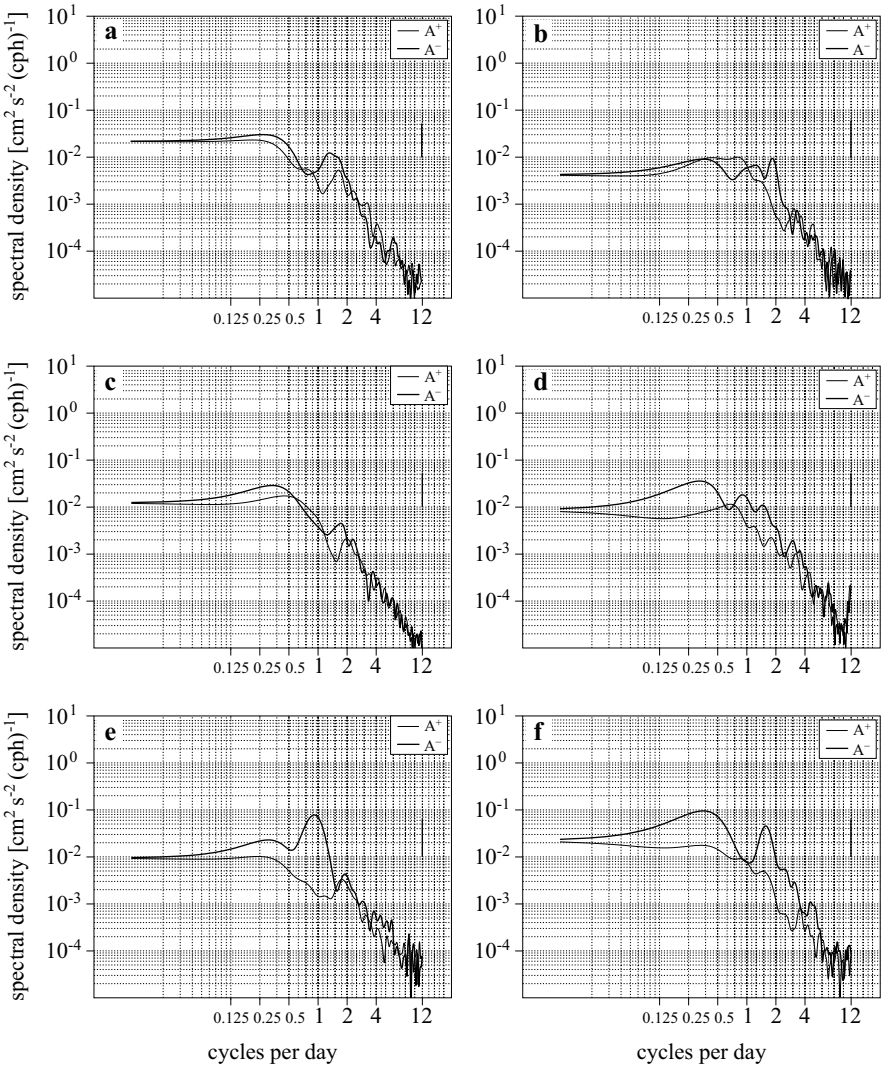

Fig. 11. Rotary spectra from the mixed layer for stations 3 (a), 4 (b), 5 (c), 6 (d), 10 (e) and 13 (f); PEX 1986. The bold line is the spectrum for the anticyclonic rotation, the solid line is the spectrum for the cyclonic rotation. The 95% confidence interval is shown as a vertical bar

salinity fronts were distinguishable also in the vertical. Fronts in the temperature were weak and not persistent; see also Eilola (1997) for a thorough description.

Winds during PEX were measured near station 5, and were generally very weak both before and during PEX. The mean wind speed was 3.8 m s^{-1}, the standard deviation 1.9 m s^{-1}.

Fig. 10 shows the u- and v-velocities from 10 m depth at the seven PEX stations. Filtering has shown that the oscillations occur in packages, but this can be seen quite clearly even in the unfiltered data, for instance at station 3 or 13. Other current components are visible, but no systematic motion was observed.

Fig. 11 shows the rotary spectra from all stations but station 8. All stations have a peak at the near-inertial band. The near-inertial signal is low at station 5, but very broad at station 6. At station 10, the largest peak is found close to 1 cycle per day instead of at the inertial frequency. Note that station 10 has a water depth of 25 m and is the shallowest of the stations.

In some of the unfiltered spectra not shown here, a heightened energy level at sub-inertial frequencies was found. This peak was much smaller than the indicated 95% confidence interval. At station 13, energy levels in the anticyclonic direction between 0.25–0.5 cycles per day were higher. Moreover, stations 3, 5 and 6 show indications of a low-frequency component in the anticyclonic spectra, but not outside the confidence interval.

Observations from PEX show that near-inertial motion existed at all stations, but less persistently than in the observations from DIAMIX and the SMHI buoy. The exception was the shallow station 10, where it was possible that the inertial oscillations were transformed into topographically trapped waves travelling around the sub-surface hill where station 10 was situated.

3.3.1. Horizontal scales

The PEX data provide the opportunity to investigate the horizontal scales of the inertial oscillations. The coherence and phase between the co-rotating spectra (between the velocity vectors rotating in the same direction) are calculated according to Mooers (1973). Fig. 12 shows the coherence and phase in the anticyclonic part of the motion between stations 13 and 3 (a), and 13 and 5 (b). The coherence between the other pair of stations is similar to Fig. 12b. The coherence of inertial oscillations will be seen for anticyclonic rotation on frequency ≈ 1.6–1.7.

Fig. 12 a shows that there is a coherence ($\approx$ 0.5) on the near-inertial band between stations 13 and 3, with a $\pi/2$ phase difference. There is no such coherence between stations 13 and 5, nor between any of the other stations. Stations 13 and 3 are the two closest stations, only 9 km apart. Station 13 and 5, which are 30 km apart, are non-coherent.

Probably because of the very weak winds, the overall velocities and the energy in the inertial oscillations are low, which limits the coherence analysis. Stations 13 and 3 have a weak coherence on the inertial frequency,

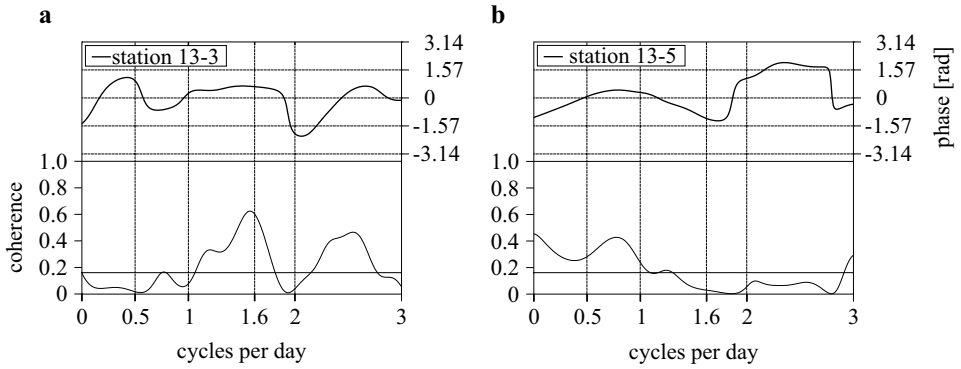

Fig. 12. Coherence and phase difference for the anticyclonic frequency between the Pex stations 13 and 3 (a) and 13 and 5 (b). The coherence is statistically significant above the solid line in the coherence plot

i.e. the oscillations observed there are coherent. Since rotor current meters, and not ADCP, were used in PEX, the measurements may have been biased by the threshold value that the rotor meters could measure.

4. Model data

Six months of data (May–October 2002) from a 3-D eddy-resolving model by Lehmann (1995) were analyzed. The model is forced by realistic atmospheric conditions taken from the SMHI meteorological data base, which covers the whole Baltic drainage basin on a regular grid of $1 \times 1°$. The temporal increment of the data is 3 hours. The model itself has a horizontal resolution of 0.045° in the north-south direction, and 0.09° in the west-east direction. The model has a vertical resolution of 3 m in the upper 100 m.

The hydrography in the model data has a shallow summer thermocline compared to the buoy data. The model perennial halocline is sharper than in the measured profiles. Otherwise, the depth of the halocline and the deepening of the seasonal thermocline compare well with observations. The anticyclonic component of the rotary spectra for 4.5 and 16.5 m depth for the second half of the period is shown in Fig. 13 together with the spectra from 4 and 16 m depth from the SMHI buoy from the period August–October 2002. The inertial oscillation is well simulated by the model, and at 4.5 m depth (a) the energy in the inertial oscillations is similar to the observed values. At 16 m, the energy on the inertial frequency is markedly smaller in the model than at the buoy. The total energy in the model spectra is one order of magnitude lower than in the observed spectra. The low energy may be due to a high model diffusivity, which removes kinetic energy faster than in the ocean. The coherence in the inertial band between this grid cell

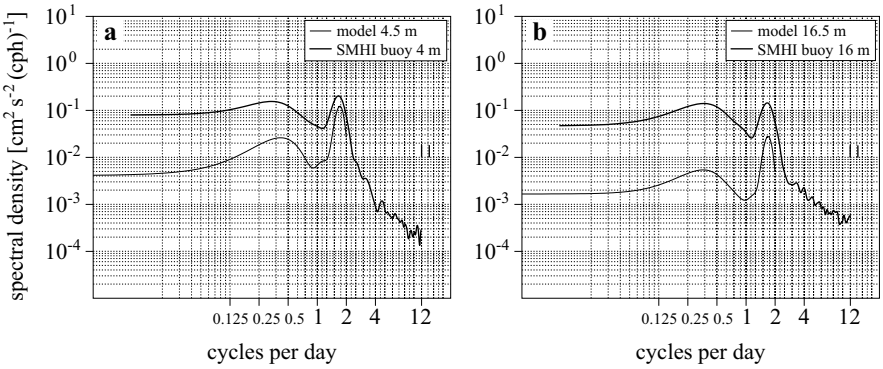

Fig. 13. The anticyclonic spectra in the model (solid line) and at the SMHI buoy (bold line). Fig. (a) shows the model depth 4.5 m, and the buoy depth 4 m, Fig. (b) shows the model depth 16.5 m and the buoy depth 16 m. The confidence interval for both the model and the buoy spectra are plotted as vertical bars in the figures

and the adjacent grid cells is very high compared to the PEX data. Large coherences are also found at other frequencies. In general, the model data are too well ordered with respect to both cyclonic and anticyclonic rotating components, as compared to observations.

The most marked qualitative difference between the model and the observed data is that the model data are too smooth, and the energies in the velocity spectra are too low. Horizontal dispersion is the result of inhomogeneities in the flow. The absence of gradients in both hydrography and velocity obviously makes the 3-D data available at present unsuitable for simulations of horizontal dispersion.

5. Summary and discussion

Current and hydrographic data from different areas of the Baltic Proper were analyzed with the aim of finding the scales in time and space that are dominant under different conditions. In our data sets, only inertial oscillations can be found at all times. Table 1 shows the total energy, E_T, of the time series, together with the energy in the inertial frequency band (1–2 cycles per day), E_I, and the ratio E_I/E_T, as a percentage. The energy in the inertial oscillations varies over three orders of magnitude. The total energy, found by integration over all frequencies, and equal to the kinetic energy per unit mass of the series, varies over two orders of magnitude. The energy in the 3-D model is comparable to the PEX measurements, but is one order of magnitude smaller than the buoy data from the same period. The total energy and the energy on the inertial band is very large in two of the

DIAMIX years, 1998 and 2000. During shorter periods, the energy on the inertial band at the SMHI buoy is comparable to these high DIAMIX levels, for instance, in the period between day 170 and 180 2003, where $E_I = 180$. The energy on the inertial band is between 10 and 20% of the total energy, with the exception of the SMHI buoy summer 2003, and DIAMIX 1998 and 2000, where it exceeds 50%. The largest fractions are found in conditions with very small mean currents.

Table 1. Total energy, E_T, for the spectra, estimated energy in the inertial oscillations, E_I, for each of the current records and the fraction E_I/E_T (percentage)

Dataset	Total energy E_T [cm s^{-1}]^2	Inertial energy E_I [cm s^{-1}]^2	E_I/E_T [%]
SMHI Aug-Oct 2002	111	17	15
SMHI June-Aug 2003	98	51	52
SMHI Oct-Nov 2003	88	10	11
DIAMIX May 1997	119	19	16
DIAMIX Jan 1998	292	205	70
DIAMIX Feb 1999	370	34	9
DIAMIX Sept 2000	355	190	54
PEX 1986	8–10, 28 (stn 13)	0.5–1.8, 3.6 (stn 13)	6–14, 17 (stn 3)
3-D model 2002	8.3	5.5	66

Inertial oscillations. The current data from the SMHI buoy, DIMIX and PEX reveal that inertial oscillations are not only a common and persistent feature, but that they occur during the whole year, under quite different stratification and wind conditions. The data indicate that inertial oscillations in the surface mixed layer are affected by both the thickness of the layer and the presence of a mean current. Without speculating on the possible energy transfer mechanisms involved, if other current components prevent the build-up or assist the breakdown of inertial oscillations, this may be one reason why inertial oscillations are common in the Baltic Proper, with its weak mean circulation and lack of tides.

PEX was special in that the winds were very weak both before and during the experiment. Inertial oscillations are found in nearly all PEX records at one time or another, although the mean energy at the inertial frequency at e.g. stations 5 and 6 is low, and the peak at station 6 very broad. At the shallow station 10, the spectra showed oscillations at frequencies around 1 cycle per day. In the PEX measurements, the two closest stations were coherent on the inertial frequency, but other adjacent

stations further apart were not. Other observations show horizontal coherence on scales from 10–20 km (e.g. Kundu 1976, Kunze & Sanford 1984, Qi et al. 1995). It seems likely that the length scale of horizontal coherence of inertial oscillations in the Baltic and other ocean areas varies depending on the prevailing conditions. First of all, the horizontal scale of the wave field will be set by the forcing. The large-scale wind field or current field (e.g. an oscillating front) initiating the inertial oscillations will also determine what the horizontal characteristics are. Once formed, the inertial oscillations are modified through different mechanisms removing energy and giving a shift in frequency (transfer to near-inertial oscillations). Some of the factors that necessarily are responsible for changing the wave are the background current and the horizontal and vertical density gradients. D'Asaro (1989) put forward the idea that the gyre-scale and mesoscale variations in velocity may lead to small-scale inertial motions. Gradients may affect motion, e.g. by modifying internal waves. It seems a reasonable assumption that the coherence scale is a quantity which varies with the properties of the forcing of the inertial oscillations and the conditions in the surrounding environment. The coherence length scale during PEX is near 10 km, which is the shortest distance between two moorings. The inertial oscillations found in PEX are the least energetic of the oscillations in our data sets. More direct measurements are needed to investigate the coherence length scale further.

Eddy and other scales. Even though other velocity components in the current meter and ADCP time series are found, these scales are not found as clearly periodic signals in the spectra. There are low-frequency motions both at the SMHI buoy site in the North-West Baltic Proper, and the DIAMIX data from the Gotland Basin on 0.25–0.5 cycles per day, allthough there is no discernible single frequency with increased amplitude. This motion could very well be due to transient eddies which, for a certain period, yield semi-periodic behavior in the spectra, and several eddies centered at the halocline were observed during DIAMIX (Stigebrandt et al. 2002). The spectra indicate that the energy in these 'transients' is of the same magnitude as the inertial oscillations occurring during the same period.

The sub-inertial oscillation observed at PEX station 10 is possibly caused by a topographically trapped wave travelling around the sub-surface hill above which station 10 is situated. The subinertial wave may have been generated by inertial oscillations interacting with the hill.

The results presented above show that two kinds of motion prevail in the open Baltic Proper and may be important sources for horizontal shear: inertial oscillations, and low-frequency or transient motions like eddies. Since these motions are predominant and non-coherent, they provide

a constant source of current shear. Fig. 14 shows the information on the dominant time and length scales in the open Baltic Proper. The stars represent inertial oscillations with different coherence scales, and the period is near 14 hours in the diagram. It is likely that the length scale of coherence can vary with mechanisms proposed above, but more knowledge is needed on how the forcing, current field and stratification affect the oscillations. The second length scale of importance is the length scale of meso-scale eddies and basin modes, which may or may not be periodic during a limited time period in one area. The diamonds are the proposed, arbitrarily chosen eddy meso-scales. The circle represents the small-scale gradients in the density field, found from hydrographic measurements in DIAMIX. Fig. 3 indicates that the large-scale gradients with length scales of the order of 100 km changes over a time scale of months.

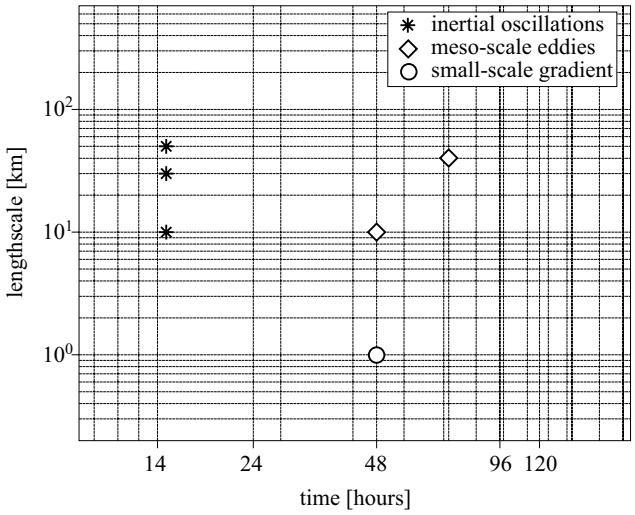

Fig. 14. A diagram of the different important length- and time-scales in the Baltic Proper. The stars show the proposed length scales of coherence for the inertial oscillations. The diamonds suggest eddy meso-scales. The circle shows the small-scale density gradients

Model data. Inertial oscillations were also found in the output from a 3-D eddy-resolving model of the Baltic. The model spectra contain too little energy on the inertial frequency and even less energy on other frequencies compared to the measurements. It was also observed that the currents are too coherent, both in the vertical and the horizontal, as compared to the available data. The objective of the observation-model comparison is to establish whether 3-D models reproduce a realistic horizontal current field that can be used to calculate horizontal dispersion.

Because of the smooth gradients both in hydrography and velocity, model data are at present not useful for horizontal dispersion studies, where gradients in the velocity field are critical. The problem probably arises both from the parameterization of sub-grid processes and the resolution of models, and needs to be solved differently in order to better represent dispersive processes.

Hydrography. The hydrography shows that the large-scale mean salinity gradient is around 0.5 per 100 km in the north-south direction; 0.005 per km. The small-scale salinity gradients in DIAMIX are 0.05 per km in the area of strongest gradient, the same as the largest gradient during PEX. Temperature gradients are also present in the measurements, but although the daily fluctuations are large, the long-term average is small.

6. Concluding remarks

The dominant time and length scales in the Baltic Sea have been evaluated, determining the important scales for the observed horizontal dispersion (Eilola & Stigebrandt 1998). Inertial oscillations and basin-scale modes are the two types of motion mostly present in the central parts of the basin. The length scale of coherence of inertial oscillations is near 10 km in our data, consistent with e.g. Kundu (1976). It seems likely that the characteristic length scale in the Baltic will vary with the amplitude of the oscillations, the wind field that is creating and breaking them down, vertical stratification and the horizontal density field. A first approximation of the horizontal shear is U/L, and for a velocity of 10 cm s^{-1} over a coherence length scale of 10 km, the shear is 10^{-5} s^{-1}. Further investigations, whether theoretical, modelling efforts, or measurements, will be of interest.

The coupling between the empirical relations and the velocity field which ultimately drives the dispersion has never been discovered. It is common to argue that the increase in apparent diffusivity is due to the fact that as the tracer cloud grows, larger and larger scales of motion will act on the particle pair or the concentration at hand. This paper has sought to better understand the processes through which this shear arises in the Baltic Proper. If the dominant process behind the observed dispersion is a shear with a length scale of tens of kilometers, a larger tracer cloud will not show the increased dispersion. Instead of a tracer cloud limitation, a coherence scale limitation will be imposed on the apparent diffusivity. However, any basin scale circulation will introduce a larger scale of motion enabling the smaller-scale current shear to act, and the relative importance of different processes interacting needs to be further assessed.

Fig. 15 summarizes what is now known about energy distribution on horizontal scales in the central Baltic Proper. The length scale of eddies is

partly a guesstimate, based on satellite images showing eddies in for instance plankton blooms, but some facts were obtained in DIAMIX and other experiments. If the true wavenumber spectrum for motion in the Baltic Proper has the shape proposed in Fig. 15, and the frequency spectrum is known, it is possible to improve dispersion modelling by utilizing a relatively simple model reproducing these properties. This is one of the targets for the future.

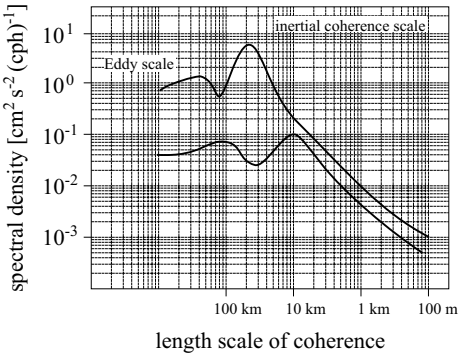

Fig. 15. Assumed energy spectra for the length scale of coherence in the Baltic. The suggested spectrum at low energies has weak inertial oscillations and a small length scale of coherence. The suggested spectrum at high energies has a larger length scale of coherence. Meso-scale eddy energy is also present in the spectra

Acknowledgements

Data was kindly provided by B. Sjöberg at SMHI, Bengt Liljebladh (DIAMIX) and Harry Dooley at ICES (PEX). A. Lehmann was very helpful providing model data. Thanks are also due B. Sjöberg for his role as sounding board. A. Stigebrandt is greatly acknowledged for his constructive ideas and help with the manuscript. The author is also grateful for the thorough and constructive comments from an anonymous reviewer.

References

Bowden K. F., 1965, *Horizontal mixing in the sea due to a shearing current*, J. Fluid Mech., 21, 83–95.

D'Asaro E. A., 1989, *The decay of wind-forced mixed layer inertial oscillations due to the β effect*, J. Geophys. Res., 94 (C2), 2045–2056.

D'Asaro E. A., Eriksen C. C., Levine M. D., Niiler P., Paulson C. A., Meurs P. V., 1995, *Upper-ocean inertial currents forced by a strong storm. Part I: Data and comparisons with linear theory*, J. Phys. Oceanogr., 25, 2909–2936.

Drinkwater K. F., Loder J. W., 2001, *Near-surface horizontal convergence and dispersion near the tidal-mixing front on northeastern Georges Bank*, Deep-Sea Res. Pt. II, 48, 311–339.

Eilola K., 1997, *Development of a spring thermocline at temperatures below the temperature of maximum density with application to the Baltic Sea*, J. Geophys. Res., 102 (C4), 8657–8662.

Eilola K., Stigebrandt A., 1998, *Spreading of juvenile freshwater in the Baltic Proper*, J. Geophys. Res., 103 (C12), 27795–27807.

Emery W. J., Thompson R. E., 1997, *Data analysis methods in physical oceanography*, 2nd edn., Elsevier, Amsterdam, 638 pp.

Fennel W., Seifert T., 1995, *Kelvin wave controlled upwelling in the western Baltic*, J. Marine Syst., 6, 289–300.

Fennel W., Seifert T., Kayser B., 1991, *Rossby radii and phase speeds in the Baltic Sea*, Cont. Shelf Res., 11 (1), 23–36.

Fonselius S., 1996, *Västerhavets och Östersjöns oceanografi*, SMHI publ., SMHI, Norrköping, 200 pp.

Gonella J., 1972, *A rotary component method for analyzing meteorological and oceanographic vector time series*, Deep-Sea Res., 19, 833–846.

Gustafson T., Kullenberg G., 1933, *Inertia currents in the Baltic*, Nature, 131 (3312), 586–587.

Herterich K., Hasselmann K., 1982, *The horizontal diffusion of tracers by surface waves*, J. Phys. Oceanogr., 12, 704–711.

Holt J. T., Proctor R., 2001, *Dispersion in shallow seas*, [chap. in:] *Encyclopedia of ocean sciences*, J. H. Steele, S. A. Thorpe & K. K. Turekian (eds.), Vol. 2, pp. 742–747, Acad. Press, San Diego.

ICES, 1989, *Baltic Sea patchiness experiment – PEX '86*, ICES Coop. Res. Rep. No 163., Vols. 1 & 2.

Joseph J., Sendner H., 1958, *Über die horizonale Diffusion im Meere*, Dt. Hydrogr. Z., 11 (2), 49–77.

Kolmogorov A. N., 1941, *On degeneration (decay) of isotropic turbulence in an incompressibla viscous liquid*, Dokl. Nauk. SSSR, 31, 538–540.

Kullenberg G., 1972, *Apparent horizontal diffusion in stratified vertical shear flow*, Tellus, 24 (1), 17–28.

Kundu P. K., 1976, *An analysis of inertial oscillations observed near Oregon coast*, J. Phys. Oceanogr., 6, 879–893.

Kunze E., Sanford T. B., 1984, *Observations of near-inertial waves in a front*, J. Phys. Oceanogr., 14, 566–581.

Lawrence G. A., Ashley K. I., Yonemitsu N., Ellis J. R., 1995, *Natural dispersion in a small lake*, Limnol. Oceanogr., 40 (8), 1519–1526.

Lehmann A., 1995, *A three-dimensional baroclinic eddy-resolving model of the Baltic Sea*, Tellus, 47, 1013–1031.

Lehmann A., Krauss W., Hinrichsen H.-H., 2002, *Effects of remote and local atmospheric forcing on circulation and upwelling in the Baltic Sea*, Tellus, 54 A, 299–316.

Levine M. D., Zervakis V., 1995, *Near-inertial wave propagation into the pycnocline during ocean storms: Observations and model comparison*, J. Phys. Oceanogr., 25, 2890–2908.

Liljebladh B., Stigebrandt A., 2000, *The contributions from the surface layer via internal waves to the energetics of deepwater mixing in the Baltic.*, Part of Ph. D. thesis, B. Liljebladh, Göteborg Univ.

McClimans T. A., Johannessen B. O., 1998, *On the use of laboratory ocean circulation models to simulate mesoscale (10–100 km) spreading*, Environ. Modell. Software, 13, 443–453.

Mooers C. N. K., 1973, *A technique for the cross spectrum analysis of pairs of complex-valued time series, with emphasis on properties of polarized components and rotational invariants*, Deep-Sea Res., 20, 1129–1141.

Okubo A., 1971, *Oceanic diffusion diagrams*, Deep-Sea Res., 18, 789–802.

Okubo A., Carter H. H., 1966, *An extremely simplified model of the 'shear effect' on horizontal mixing in a bounded sea*, J. Geophys. Res., 52–67.

Peeters F., Wuest A., Piepke G., Imboden D. M., 1996, *Horizontal mixing in lakes*, J. Geophys. Res., 101 (C8), 18361–18375.

Pollard R. T., 1970, *On the generation by winds of inertial waves in the ocean*, Deep-Sea Res., 17, 795–812.

Qi H., de Scoeke R. A., Paulson C. A., Eriksen C. C., 1995, *The structure of near-inertial waves during ocean storms*, J. Phys. Oceanogr., 25, 2853–2871.

Raudsepp U., Beletsky D., Schwab D. J., 2003, *Basin-scale topographic waves in the Gulf of Riga*, J. Phys. Oceanogr., 33, 1129–1140.

Sanderson B. G., Okubo A., Webster I. T., Kioroglou S., Appeldoorn R., 1995, *Observations and idealized models of dispersion on the southwestern Puerto-Rican insular shelf*, Math. Comp. Modelling, 21 (6), 39–63.

Schott F., Ehlers M., Hubrich L., Quadfasel D., 1978, *Small-scale diffusion experiments in the Baltic surface-mixed layer under different weather conditions*, Dt. Hydrogr. Z., 31 (6), 195–215.

Stigebrandt A., 2001, *Physical oceanography of the Baltic Sea*, [in:] *A systems analysis of the Baltic Sea*, F. Wulff et al. (eds.), Springer-Verl., Berlin-Heidelberg, 19–74.

Stigebrandt A., Lass H.-U., Liljebladh B., Alenius P., Piechura J., Hietala R., Beszczynska A., 2002, *Diamix-an experimental study of diapycnal deepwater mixing in the virtually tideless Baltic Sea*, Boreal Environ. Res., 7, 363–369.

Young W. R., Rhines P. B., Garrett C. J. R., 1982, *Shear-flow dispersion, internal waves and horizontal mixing in the ocean*, J. Phys. Oceanogr., 12, 515–527.